Experimental Investigation of the Optimal Ingot Resistivity for both the Cell Performances and the Temperature Coefficients for Different Cell Architectures

Charly Berthod[1], Sissel Tind Søndergaard[1], and Jan Ove Odden[2]

[1]University of Agder, P.O. Box 509, NO-4898 Grimstad, Norway,
[2]Elkem Solar AS, P.O. Box 8040 Vaagsbygd, NO-4675 Kristiansand S, Norway

***Abstract*—Compensation engineering enables the achievement of lower ingot resistivities with relatively constant performances along the ingot height. In this paper the impact of the bulk resistivity on the cell performances and the temperature coefficients is investigated for compensated and non-compensated multicrystalline silicon. Based on experimental data we show that reducing the bulk resistivity below a certain value improves the temperature coefficients but deteriorates the cell performances for two distinct cell architectures (Al-BSF and PERCT). Moreover this performance loss is not balanced out by the improved temperature coefficient for operating conditions below 70 °C.**

***Index Terms*—multicrystalline silicon, bulk resistivity, temperature coefficient, photovoltaic cells.**

I. Introduction

Multicrystalline silicon (mc-Si) represents more than 60 % of the world's market in PV technologies [1]. The most produced solar cell type is conventional p-type mc-Si Aluminum Back Surface Field (Al-BSF) due to its manufacturing simplicity and low cost. However standard casted ingots are predicted to be replaced by high performance multicrystalline ingot (HP multi) in the coming years. It is explained by the smaller grain sizes that decrease the stress during crystal growth causing a reduction in dislocation densities thus an improvement in cell performances [2]. Another major industry change happening these years is the shift from Al-BSF cells to PERC (Passivated Emitter and Rear Cell) with the addition of a few processing steps in the production line that improve the passivation of the rear side. This enhanced passivation causes an absolute gain in cell conversion efficiency over 1 % [3] and explains the rapid transition from Al-BSF to PERC which is expected to be the dominant cell production technology by 2020 [1]–[4].

Modeling solar cell performances for different cell architectures has received a lot of attention recently [4]–[8]. The lifetime distribution, the resistivity and the dislocation density for mc-Si are the key parameters that are used to predict the solar cell performances. A high resistivity was shown to improve the cell performances for most cell architectures, except for some PERC designs where 3D carrier transport was happening [5]. Yet another study has shown that these results are to be considered cautiously as the lifetime limiting impurities present in the material have a great influence on the dependence of the cell efficiency with the resistivity [6].

In this paper an experimental investigation of the optimal resistivity is carried out. First, compensation engineering is shown to be a suitable method to reach lower resistivities with an enhanced resistivity control along the height of the brick. Then the effect of the brick resistivity on the cell performances and the temperature coefficients for two different cell architectures is presented. Finally, we compare the brick-averaged cell efficiencies from 25 to 70 °C to determine which brick resistivity gives the best cell performances at a temperature closer to real operating conditions.

II. Experimental Details

In this study, four HP-multi G5 ingots were cast. One reference ingot in polysilicon with a targeted resistivity of 1.3 Ω cm, and three ingots made of compensated silicon (with 70 % of Elkem Solar Silicon (ESS^{TM}) and 30 % of polysilicon) with distinct targeted resistivities. The phosphorus concentration is the typical concentration found in ESS^{TM}after the purification steps. The same amount of gallium is added in all compensated ingots and the boron concentration is varied to obtain the targeted resistivities. The description of the ingots with their initial dopant concentrations in the silicon melt (from Ref [9]) is presented in Table 1.

A center brick from each ingot was cut into wafers that were divided into two groups. All wafers were processed into cells in a research line. The first group of wafers underwent a standard Al-BSF cell process while the other wafers were processed as PERCT (Passivated Emitter Rear Totally diffused) cells with a full area back surface field made by a BBr_3 boron diffusion step in a standard diffusion tube furnace - prior to the back side passivation and protection by a PECVD SiN_x (a detailed description of the full process is available in Ref. [10]). A minimum of 9 cells per brick were selected evenly along the brick height to ensure a full brick height coverage.

The solar cells were light-soaked to ensure a full degradation of the BO defect and then their current-voltage (IV) characteristics were measured under a standard AM1.5G spectrum with a NeonSee^{TM}AAA sun simulator. The temperature coefficients of a cell were obtained by measuring several IV characteristics from 25 °C to 70 °C to get the cell parameters at all temperature steps. Then a linear fitting over the temperature range is performed for each parameter

TABLE 1

DESCRIPTION OF THE INGOTS

Ingot name	Blend-in-ratio (% ESS^{TM})	Targeted resistivity (Ω cm)	Dopant concentrations (cm^{-3})		
			P	B	Ga
Comp 0.5	70	0.5	1.9×10^{16}	5.2×10^{16}	1.6×10^{17}
Comp 0.9	70	0.9	1.9×10^{16}	3.0×10^{16}	1.6×10^{17}
Comp 1.3	70	1.3	1.9×10^{16}	2.4×10^{16}	1.6×10^{17}
Ref 1.3	0	1.3	-	1.3×10^{16}	-

before dividing by the cell parameters value at 25 °C to obtain the relative temperature coefficient of this parameter. In this study temperature coefficients generally relates to relative temperature coefficients unless otherwise stated.

III. Results and Discussion

A. Resistivity Profiles

The resistivity profiles of the center bricks measured by Semilab Eddy current testing are plotted in Fig 1. The three dopants have segregation below one therefore they will segregate at the top of the ingot. The relative height represents the solidification fraction after bottom and top cuts. The reference ingot displays the general decreasing resistivity profile caused by the increase in boron concentration along the ingot height. One can note that to obtain an average resistivity of 1.3 Ω cm, the resistivity at the bottom of the ingot must start at a higher value. Concerning the compensated ingots, their resistivity profiles are more complex as compensation engineering was used with the addition of gallium. The two main advantages of tri-doping are a better resistivity control and the avoidance of a p/n changeover near the top of the ingot which happens when only boron and phosphorus are present [11], [12]. Both ingots *Comp 0.5* and *Comp 0.9* have notable even resistivity profiles enabled by compensation engineering. However, the resistivity profile of *Comp 1.3* increases considerably at the top part showing the sensitivity of compensation engineering. This gives rather symmetrical resistivity profiles along 1.3 Ω cm for *Ref 1.3* and *Comp 1.3* with a crossing resistivity near 60 % of the relative height. Gallium starts being the dominant dopant in the very top part of the ingot which decreases dramatically the resistivity [9]. This is not shown in Fig. 1 because this part of the ingot is always cut to remove the segregated impurities.

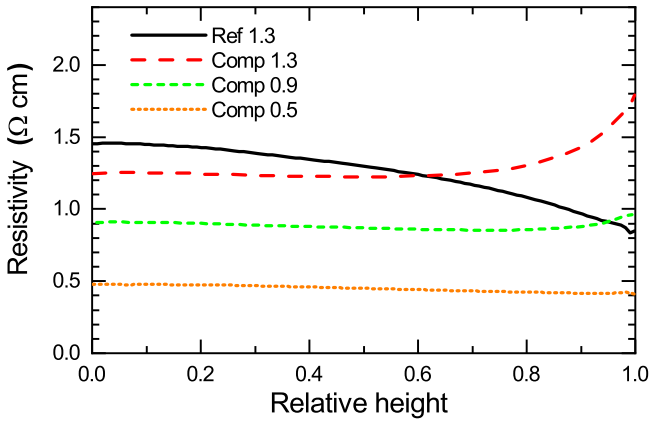

Fig. 1. Resistivity profiles of the center bricks of the four ingots measured by Semilab Eddy current testing.

B. Open-circuit voltage

In Fig. 2a) the mean values of the open-circuit voltage (V_{oc}) and their 95 % confidence intervals for each ingot are plotted. PERC cells have their V_{oc} approximately 10mV higher than the Al-BSF cells as a consequence of the improved back surface passivation. PERC cells present larger variations for each ingot and this can be explained by a higher attainable open-circuit voltage offered by this cell architecture which makes them more sensitive to the carrier lifetime fluctuations along the brick height [5]. Ingot *Comp 0.5* has an even larger confidence interval than *Comp 1.3* and *Comp 0.9*, and as explained in Ref. [13] it arises from the higher initial boron

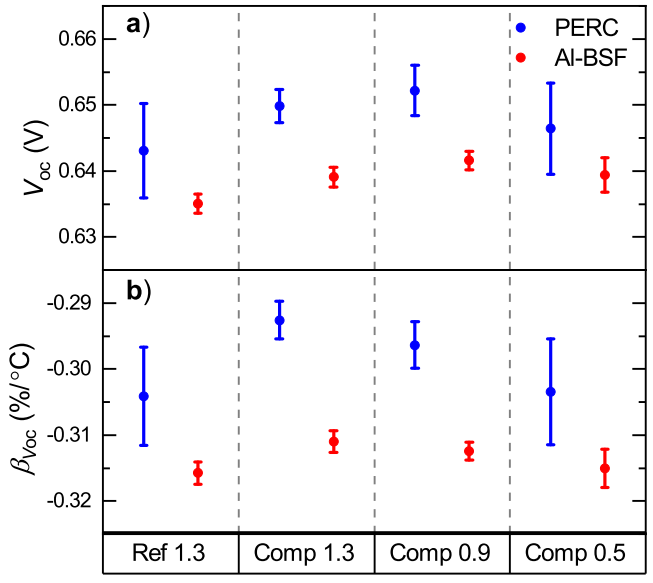

Fig. 2. Mean values of a) V_{oc} at 25 °C and b) $\beta_{V_{oc}}$ and their 95 % confidence intervals for the four ingots. The PERC cells are in blue and the Al-BSF cells in red.

concentration. This causes a reduced lifetime and increased dopant density at the top of the ingot due to segregation which reduces significantly the cell performances in this part of the ingot, resulting in larger variations along the ingot height. Ingot *Ref 1.3* shows lower V_{oc} than *Comp 1.3* for both cell architectures, which is not something usually encountered by the ingots producer (REC Solar). Therefore, we suppose it originates from fluctuations in the solidification process from ingot to ingot. The ingot resistivity does not have a large impact on V_{oc}, and both cell architectures obtain their best V_{oc} for an ingot resistivity of 0.9 Ω cm.

In Fig. 2b) the mean values of the temperature coefficient of the open-circuit voltage ($\beta_{V_{oc}}$) and their 95 % confidence intervals for each ingot are plotted. This coefficient can be expressed as a function of V_{oc} (from Ref. [14]):

$$\beta_{V_{oc}} = -\frac{1}{V_{oc}T_c}\left(\frac{E_{g0}}{q} - V_{oc} + \gamma\frac{kT_c}{q}.\right) \quad (1)$$

where T_c is the cell temperature, E_{g0} is the extrapolated bandgap at 0 K, q is the electron charge, γ is a parameter describing the behavior of the recombination mechanisms with temperature and k Boltzmann constant. Both graphs in Fig. 2 are very similar as a result of the quasi-linear dependence of $\beta_{V_{oc}}$ with V_{oc}. PERC cells have the temperature coefficients closest to zero because of an enhance V_{oc}, ingots with large variations in V_{oc} have large variations in $\beta_{V_{oc}}$. The only noticeable difference is that the ingot with the highest temperature coefficient is *Comp 1.3* and not *Comp 0.9* as would be expected from its higher V_{oc}. We observe that lowering the resistivity has a negative impact on this temperature coefficient, for both cell architectures. As this is in contrary with the results on V_{oc}, this means that there is a sensible difference in the value of γ for solar cells with different base resistivities. In a previous study with the same feedstocks but a different PERC cell architecture [15], both V_{oc} and $\beta_{V_{oc}}$ were found to increase when lowering the resistivity. This means that the optimal resistivity depends strongly on the cell design. This is especially important for the PERC cells where the presence, or not, of a totally-diffused layer at the rear side (like the cells studied here) have a substantial impact on the optimal resistivity [5].

C. Short-circuit current

In Fig. 3a) the mean values of the short-circuit current (I_{sc}) together with their 95 % confidence intervals for each ingot are plotted, similarly for the temperature coefficient of the short-circuit current ($\beta_{I_{sc}}$) in Fig. 3b). The impact of the improved passivation on the rear-side of the PERC cells is seen in the I_{sc} difference between the two cell architectures of approximately 0.5 A. Ingot *Ref 1.3* presents a lower current compared to *Comp 1.3*, which is also assumed to originate from fluctuations in the solidification process. There is not a significant difference of current between the ingots *Comp 1.3* and *Comp 0.9*, however the ingot *Comp 0.5* suffer from

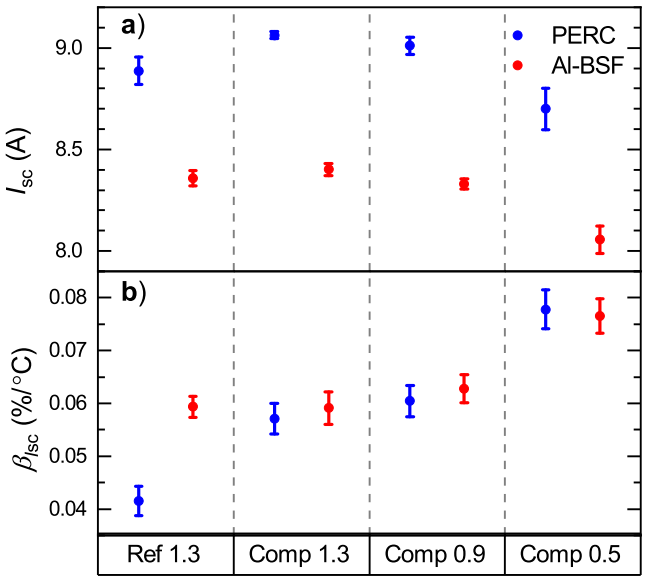

Fig. 3. Mean values of a) I_{sc} at 25 °C and b) $\beta_{I_{sc}}$ and their 95 % confidence intervals for the four ingots. The PERC cells are in blue and the Al-BSF cells in red.

severe current losses compared to the previous two, for both cell types.

In Fig. 3b) we observe that both PERC and Al-BSF solar cells present similar temperature coefficients, except for the ingot *Ref 1.3*. The PERC cells of this ingot have an abnormally low $\beta_{I_{sc}}$ which is unexplained. The three compensated ingots show an improvement of $\beta_{I_{sc}}$ with lower resistivities already observed in Ref. [15].

D. Fill Factor

The mean values of the fill factor (FF) and its temperature coefficient (β_{FF}) and their 95 % confidence intervals are plotted in Fig. 4a) and b) respectively. The PERC and Al-BSF solar cells studied here show very similar FF. This PERC architecture has a totally diffused rear-side which improves the passivation while preventing an important increase of the series resistance which would have reduced FF [5]. The two ingots with the lowest resistivities have slightly higher FF. The three compensated ingots have similar values of V_{oc}, as observed in Fig. 2, therefore we conclude it comes from a decrease in the series resistance caused by a more conductive base.

β_{FF} can be expressed as a function of V_{oc}, from Ref. [16]:

$$\beta_{FF} = (1 - 1.02FF_0)\left(\beta_{V_{oc}} - \frac{1}{T_c}\right) - \frac{R_s}{V_{oc}/I_{sc} - R_s}\,\beta_{R_s}. \quad (2)$$

where FF_0 is the fill factor free of parasitic resistance losses (from Ref. [17]), R_s is the series resistance and β_{R_s} its relative temperature coefficient.

FF_0 and $\beta_{V_{oc}}$ increase with V_{oc} (cf. Eq. 1). As mentioned earlier, PERC and Al-BSF cells have similar FF (Fig. 2a)),

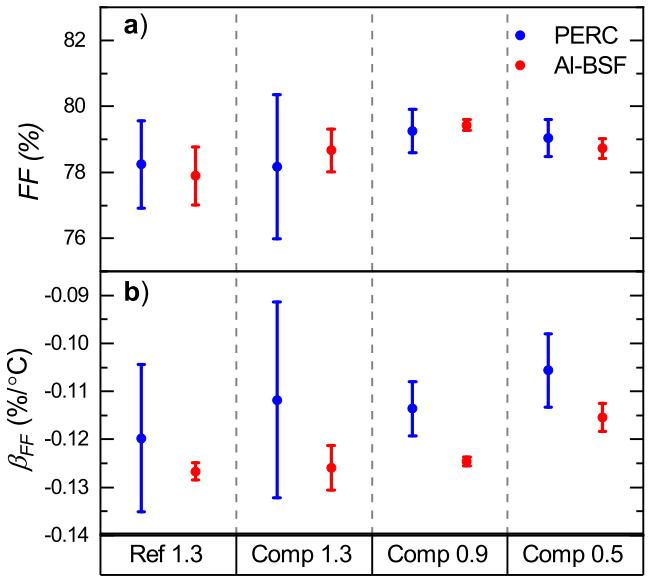

Fig. 4. Mean values of a) FF at 25 °C and b) β_{FF} and their 95 % confidence intervals for the four ingots. The PERC cells are in blue and the Al-BSF cells in red.

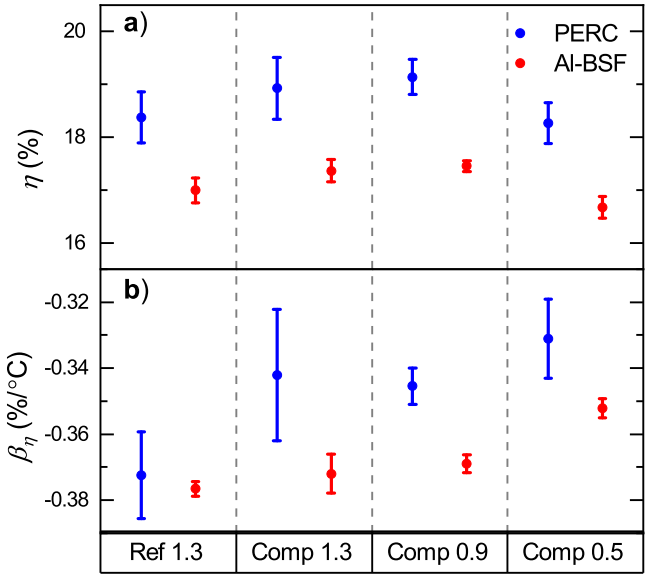

Fig. 5. Mean values of a) η at 25 °C and b) β_η and their 95 % confidence intervals for the four ingots. The PERC cells are in blue and the Al-BSF cells in red.

however PERC cells have higher V_{oc} (Fig. 1a)). This results in β_{FF} being closer to zero for the PERC cells, as observed in Fig. 4b) for the four ingots. In addition, the ingot *Comp 0.5* has the highest β_{FF}. It is explained by the lower series resistance of these cells caused by a more conductive base which positively impacts the second term in Eq. 2 [15], [18].

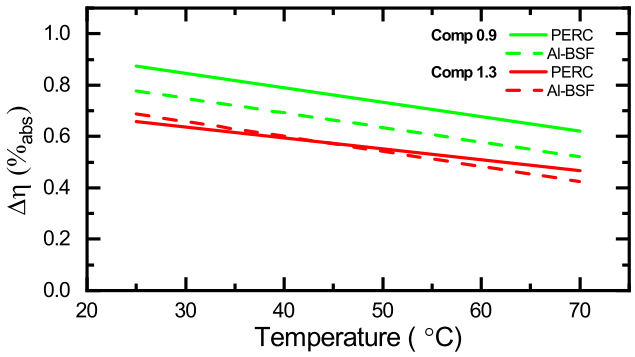

Fig. 6. Absolute differences of the efficiency mean values for ingots *Comp 1.3* and *Comp 0.9* compared to *Comp 0.5*, on PERC and Al-BSF solar cells, on the temperature range measured by the sun simulator.

E. *Efficiency*

The temperature coefficient of the efficiency β_η is the sum of the temperature coefficients of: the short-circuit current, the open-circuit voltage and the fill factor. The means values of the efficiency (η) together with their 95 % confidence intervals are plotted in Fig. 5a), similarly for β_η in Fig. 5b). PERC cells show efficiencies nearly 1 % higher for the four ingots. We observe that the ingot *Ref 1.3* show slightly lower efficiencies than *Comp 1.3* on both cell types due to the solidification step. Ingot *Comp 0.5* show a clear decrease compared to the two other compensated ingots because of the observed losses in V_{oc} and I_{sc}.

Ingot *Comp 0.5* possesses the highest temperature coefficients and the lowest efficiencies at 25 °C on both cell architectures, which is in agreement with previous studies [15], [19]. The impact of the improved temperature coefficients could be large enough so that this ingot would exhibit higher performances than the other compensated ingots at higher temperatures. In order to find out, the mean values of the efficiencies and the temperature coefficients plotted in Fig. 5 are used to calculate the absolute difference in efficiency between *Comp 1.3* and *Comp 0.5*, and *Comp 0.9* and *Comp 0.5*. The results on the temperature range used in the sun simulator are plotted in Fig. 6. We observe that both ingots have significantly better performances on the whole temperature range, for both cell types. This means that the efficiency losses due to the reduction of the base resistivity are not balanced out by the improvement of the temperature coefficient. However, reducing the resistivity from 1.3 Ω cm to 0.9 Ω cm improves the performances.

IV. Conclusion

In this article, the positive effect of improving the rear-side passivation on the cell parameters and the temperature coefficients is revealed. Tri-doping is demonstrated to be an effective method to have an enhanced control of the resistivity along the ingot, thus to achieve lower ingot resistivities

without suffering of large performances losses at the top of the ingot. Lowering the base resistivity significantly improves the temperature sensitivity of solar cells. This result is confirmed on two different cell architectures. However, it is shown that this improvement is not sufficient to counterbalance the performance losses for normal operating temperatures.

ACKNOWLEDGMENT

Funding for this work was provided through the EnergiX programme of the Norwegian Research Council, project number 256271 - Performance and Reliability IN Compensated Elkem Solar Silicon.

REFERENCES

[1] ITRPV, "International technology roadmap for photovoltaics," 8th edition, 2017.

[2] C. Lan, A. Lan, C. Yang, H. Hsu, M. Yang, A. Yu, B. Hsu, W. Hsu, and A. Yang, "The emergence of high-performance multi-crystalline silicon in photovoltaics," *Journal of Crystal Growth*, vol. 468, pp. 17–23, 2017.

[3] B. Min, M. Müller, H. Wagner, G. Fischer, R. Brendel, P. P. Altermatt, and H. Neuhaus, "A roadmap toward 24% efficient perc solar cells in industrial mass production," *IEEE Journal of Photovoltaics*, vol. 7, no. 6, pp. 1541–1550, 2017.

[4] M. A. Green, "The passivated emitter and rear cell (perc): From conception to mass production," *Solar Energy Materials and Solar Cells*, vol. 143, pp. 190–197, 2015.

[5] H. Steinkemper, M. Hermle, and S. W. Glunz, "Comprehensive simulation study of industrially relevant silicon solar cell architectures for an optimal material parameter choice," *Progress in Photovoltaics: Research and Applications*, vol. 24, no. 10, pp. 1319–1331, 2016.

[6] H. Steinkemper, B. Michl, M. Hermle, and S. W. Glunz, "Choosing the best silicon material parameters for different solar cell architectures," *Energy Procedia*, vol. 92, pp. 225–231, 2016.

[7] B. Mitchell, D. Chung, Q. He, H. Zhang, Z. Xiong, P. P. Altermatt, P. Geelan-Small, and T. Trupke, "Perc solar cell performance predictions from multicrystalline silicon ingot metrology data," *IEEE Journal of Photovoltaics*, vol. 7, no. 6, pp. 1619–1626, 2017.

[8] P. P. Altermatt, Z. Xiong, Q. He, W. Deng, F. Ye, Y. Yang, Y. Chen, Z. Feng, P. J. Verlinden, A. Liu *et al.*, "High-performance p-type multicrystalline silicon (mc-si): Its characterization and projected performance in perc solar cells," *Solar Energy*, 2018.

[9] R. Søndenå, H. Haug, A. Song, C.-C. Hsueh, and J. O. Odden, "Resistivity profiles in multicrystalline silicon ingots featuring gallium co-doping," *AIP conference proceedings*, To be published.

[10] A. Teppe, C. Gong, K. Zhao, J. Liu, S. Wang, J. Dong, S. Zhou, S. Keller, M. Klenk, I. Melnyk *et al.*, "Progress in the industrial evaluation of the mc-si perct technology based on boron diffusion," *Energy Procedia*, vol. 77, pp. 208–214, 2015.

[11] A. Cuevas, M. Forster, F. Rougieux, and D. Macdonald, "Compensation engineering for silicon solar cells," *Energy Procedia*, vol. 15, pp. 67–77, 2012.

[12] M. Forster, "Compensation engineering for silicon solar cells," Ph.D. dissertation, INSA de Lyon, 2012.

[13] H. Haug, Å. Skomeland, R. Søndenå, M. S. Wiig, C. Berthod, and E. S. Marstein, "Temperature coefficients in compensated silicon solar cells investigated by temperature dependent lifetime measurements and numerical device simulation," *AIP conference proceedings*, To be published.

[14] O. Dupré, R. Vaillon, and M. A. Green, "Physics of the temperature coefficients of solar cells," *Solar Energy Materials and Solar Cells*, vol. 140, pp. 92–100, 2015.

[15] C. Berthod, R. Strandberg, J. O. Odden, and T. O. Sætre, "Reduced temperature sensitivity of multicrystalline silicon solar cells with low ingot resistivity," in *Photovoltaic Specialist Conference (PVSC), 2016 IEEE 43rd*. IEEE, Conference Proceedings.

[16] J. Zhao, A. Wang, S. Robinson, and M. Green, "Reduced temperature coefficients for recent highperformance silicon solar cells," *Progress in Photovoltaics: Research and Applications*, vol. 2, no. 3, pp. 221–225, 1994.

[17] M. A. Green, "Solar cell fill factors: General graph and empirical expressions," *Solid-State Electronics*, vol. 24, pp. 788 – 789, 1981.

[18] O. Dupré, "Physics of the thermal behavior of photovoltaic devices," monograph, INSA de Lyon, 2015.

[19] M. Mueller, A. Schulze, J. Isemberg, B. Hund, and H. G. Beyer, "Influence of the wafer resistivity on the temperature coefficients of industrial silicon solar cells and on the expected performance behaviour," in *Prceeding of 25th EU PVSEC/WCPEC-5 conference*, 2010, pp. 2600–2603.